Simulated Data-Guided Incremental SAR ATR Through Feature Aggregation

Ziyang Tang, Yuli Sun, Chenfang Liu, Yanjie Xu, and Lin Lei

***Abstract*—Applying synthetic aperture radar automatic target recognition (SAR ATR) in open scenario based on deep learning (DL) is challenging due to the difficulty in incrementally recognizing new targets with limited samples. To address this challenge, we introduce simulated data that reflects the structure and scattering features of the new target to supplement measured data for better performance, and then, we propose a novel class incremental SAR ATR method guided by simulated data through feature aggregation (SGFA). Due to the gap between simulated and measured data, DL-model prefers extracting simulated-specific features in incremental learning, resulting in misclassification of new targets. In order to avoid the bias learning of simulated data, SGFA utilizes feature aggregation to extract scattering and structural features that are present in both simulated and measured images, which consists of measured data-anchored minibatch construction strategy (MDA) and feature-level contrastive loss. Specifically, the MDA can reduce the high sampling probability of a large number of simulated samples in each minibatch. The feature-level contrastive loss can aggregate the feature distributions of simulated and measured data, which is obtained by automatically constructing sample pairs through cyclic shifts of feature vectors in the minibatch. In addition, a small amount portion of simulated data is retained to resist severe forgetting caused by the difficulty of adequately representing the data distribution with limited measured data. The experiments on SAMPLE dataset demonstrate the effectiveness of the proposed method.**

***Index Terms*—Automatic target recognition (ATR), class incremental learning, simulation, synthetic aperture radar (SAR).**

I. Introduction

SYNTHETIC aperture radar (SAR), is an active earth observation sensor that can image the area of interest in all-day and all-weather conditions [1]. It offers unique advantages for both military and civilian applications. The development of SAR imaging technology has made it more feasible to obtain a large number of high-resolution SAR images. When presented with massive SAR data, efficient SAR automatic target recognition (SAR ATR) algorithms are urgently needed due to the low timeliness of manual interpretation alone. The powerful automatic data processing capabilities of deep learning (DL) have reinvigorated SAR ATR and advanced results have been obtained [2], [3]. These DL-based methods rely on closed-world assumptions, where the class and number of samples in the training set are fixed. However, sensors increasingly acquire new target images in open scenarios. In order to recognize new class targets, historical data are generally retrained together with new data, which results in significant time consumption and waste of storage resources.

Class incremental learning enables the continuous acquisition of knowledge of new classes while accessing minimal or no historical data, which is considered to be more suitable for open scenarios where the data is gradually increased. In recent years, numerous incremental learning algorithms have emerged due to the rapid development of this field [4], [5]. Among them, the algorithm based on preserving a small portion of old class data as exemplars is effective for preventing forgetfulness and simple to execute. Therefore, number of incremental learning methods for SAR ATR improve upon retaining old samples. For instance, HPecIL [6] utilized multimodel knowledge distillation to correct the accumulative errors of old classes, and unstructured pruning initialization to improve the plasticity of model. Dang et al. [7] proposed class boundary exemplar selection to select more diverse samples for incremental SAR ATR. Li et al. [8] proposed incremental class anchor clustering to address the confusion between the representations of new and old classes in the feature space. Li et al. [9] presented density coverage-based exemplar selection to pick those samples that can cover the class distribution to the maximum extent as exemplars. The algorithms described above produce satisfactory results on SAR benchmark datasets, such as MSTAR. However, these methods are based on the condition that the training samples of the new target are sufficient and do not consider the situation where the measured samples are limited.

In real-world scenarios, access to limited training samples for certain targets is often the norm, such as noncooperative military targets. Learning new targets incrementally under such limited training data condition can be challenging. On the one hand, the limited amount of measured data poses a challenge for the model to effectively extract information about the features of new targets. On the other hand, when processing subsequent new data, it can be difficult to avoid the model's tendency to forget this class, even if all limited measured data is retained. Although some studies have introduced prototype learning to alleviate the overfitting problem caused by limited samples [11],

Manuscript received 7 April 2024; revised 4 June 2024; accepted 20 June 2024. Date of publication 25 June 2024; date of current version 8 August 2024. This work was supported in part by the Postdoctoral Fellowship Program of CPSF under Grant GZC20233545, and in part by the Natural Science Foundation of Hunan Province of China under Grant 2024JJ6466. *(Corresponding author: Lin Lei.)*

The authors are with the State Key Laboratory of Complex Electromagnetic Environment Effects on Electronics and Information System, the College of Electronic Science and Technology, National University of Defense Technology, Changsha 410073, China (e-mail: tangziyang@nudt.edu.cn; sunyuli@mail.ustc.edu.cn; liuchenfang99@163.com; 603220383@qq.com; leilin98@nudt.edu.cn).

Digital Object Identifier 10.1109/JSTARS.2024.3418775

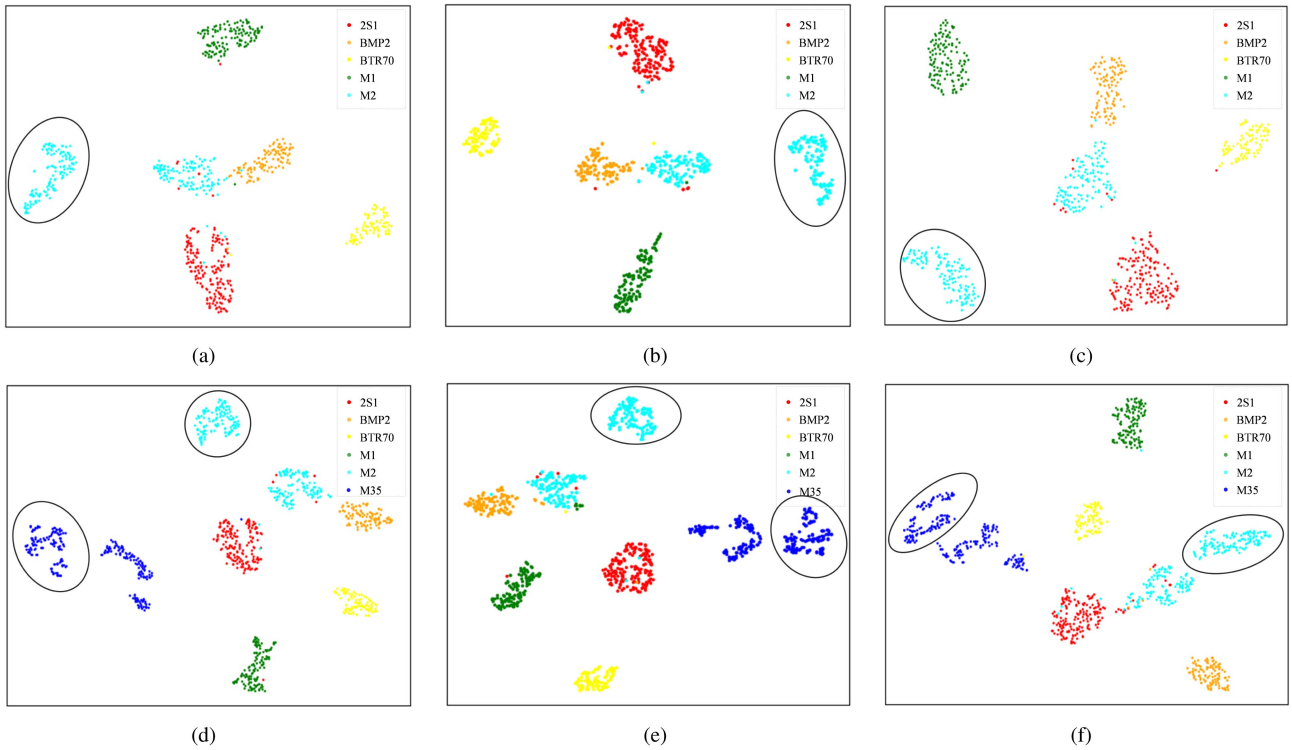

Fig. 1. Visualization results for incrementally learning 1 (Top) and 2 (Bottom) new classes using iCaRL [4], WA [5], and Replay respectively, where new classes contain small amount of measured data and sufficient simulated data from SAMPLE dataset [10]. The number of base classes is 4, and new class of each incremental task is 1. Inside the black circle are the sample points of the simulated data. (a) iCaRL-5. (b) WA-5. (c) Replay-5. (d) iCaRL-6. (e) WA-6. (f) Replay-6.

[12], sufficient data is a more effective support for DL which is a data-driven algorithm, particularly for SAR images, which are greatly affected by imaging conditions.

SAR image simulation technology is another important way to obtain SAR images. A large number of simulated images of specified target can be generated by computer aided design (CAD) model and electromagnetic calculation tools, which can well simulate the geometric and scattering feature of the target. However, simulated images are influenced by the realism of the CAD model and the accuracy of the electromagnetic calculations, which may differ from the measured data [13]. As shown in Fig. 2, there is a discernible disparity between the measured and simulated images, both in terms of the background clutter and the distribution of strong scattering points. This discrepancy ultimately results in the divergence of the two distributions in the deep feature space, as shown in Fig. 1. Numerous studies have aimed to reduce the disparities between simulated and measured data to effectively utilize simulated data for SAR ATR, and the results are positive in limited measured data [14], few-shot [15], and zero-shot [16] conditions.

The successful application of simulated data in SAR ATR inspired the introduction of simulated data into the incremental SAR ATR. In the incremental learning, sufficient simulated data can aid in the acquisition of new knowledge by providing a comprehensive and detailed characterization of the target structure. In addition, the structural and scattering features present in the simulated images exhibit better stability, which is beneficial for preserving old knowledge. However, very few scholars have conducted research on this.

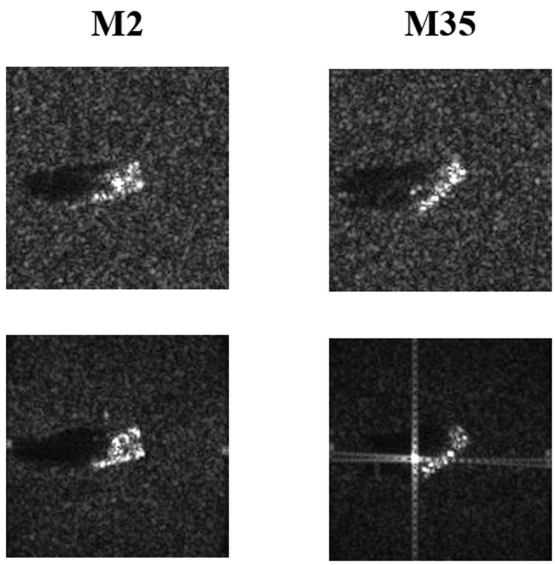

Fig. 2. Selected measured images (Top) and simulated images (Bottom) of M2 and M35.

In this article, we consider a scenario in which a model, trained on classes with ample measured data (base classes), incrementally learns new classes that contains a small amount of measured data and sufficient simulated data. Two issues were found as follows.

1) *Simulated-Feature Preference:* When directly introducing simulated data, the model may extract simulated-specific

features to achieve a high degree of separability between the new and old classes in training set. This can result in differences between the simulated and measured data in the feature space, as shown in Fig. 1. For similar target, the difference can be even greater than the difference of interclass.

2) *Catastrophic Forgetting:* Incremental learning faces the problem of forgetting-a significant decline in the ability to discriminate old classes while learning new knowledge. Although retaining a small amount of old classes data can provide some resistance to it, too little measured data for incremental classes make them more forgettable than the base classes.

In light of above issues, a novel method guided by simulated data through feature aggregation (SGFA) is proposed for SAR image class incremental learning with simulated data supplementation. Specifically, feature aggregation is performed at each minibatch to ensure that the model extracts scattering and structural features that are present in both simulated and measured images. To tackle the issue of severely forgetting incremental classes, we retain a portion of the simulated data, in addition to the measured data, to prevent forgetting. The primary contributions of this article can be induced as follows.

1) A novel class incremental SAR ATR framework guided by SAR simulated data is proposed to address the issue of limited samples for new targets. Adequate simulated data was used to supplement the limited measured data for the new classes. By aggregating the feature distribution of both, the simulated data can better guide the learning from new classes. When subsequent data arrives, a small portion of simulated data is retained to resist forgetting.
2) A feature aggregation method is proposed to avoid bias learning of simulated data, which contains measured data-anchored min-batch construction strategy (MDA) and designed feature-level contrastive loss. The MDA ensures that each minibatch contains measured data for subsequent contrastive loss calculation. The feature-level contrastive loss minimizes the Euclidean distance between simulated and measured data in each minibatch by cyclic shifts to extract their common features.
3) A herding-based selection method for simulated data is proposed to resist severe forgetting of incremental classes. It is designed to choose new classes of simulated samples to add to the exemplar set for preventing severe forgetting. To select representative simulated exemplars efficiently, We consider the center of the measured data sample as class center and then select the simulated samples that are closest to the class center in the feature space by herding.

II. Related Work

A. Incremental Learning

Class incremental learning aims to design machine learning models with continuous learning capabilities for new class data. The prevailing class incremental learning methods can be summarized at three levels: 1) data; 2) model; and 3) algorithm [17].

1) Class Incremental Learning Methods: Data-centric methods construct exemplar set for old class [18], [19] or generate pseudodata [20], [21] for participation in model updates to combat forgetting. The methods of directly retaining a small amount of old data are widely used due to their simplicity and effectiveness, despite the fact that they consume a certain amount of memory. For the latter, they rely on the quality of the pseudodata and require constant updates to the generative network, increasing requirements for algorithm design. In addition, some works utilize exemplar set to constraint optimization direction for retaining previous knowledge [22], [23]. The practical application of these methods is hindered by overreliance on unverified assumptions. Model-centric methods continuously adapt to new data by limiting updates to important parameters [24], [25] or by dynamically adjusting the network structure [26], [27]. For the former, they need to save a parameter importance matrix for each incremental task, which will linearly consume storage resources, while the parameter importance matrices of different tasks may be contradictory for model updating, impeding its evolution. Algorithms that rely on dynamic model structures require task identifiers to specify the selection of subnetworks, which can make it difficult to meet practical requirements. Algorithm-centric methods work on designing specific algorithm to maintain the model's knowledge of past tasks, such as knowledge distillation [28] and model rectify [5], [29]. Although algorithm-centric methods increase the complexity of algorithm design, they can be well integrated with the first two levels of methods [30], [31]. Therefore, they have received a lot of attention.

2) Class Incremental SAR ATR Methods: Currently, research on class incremental learning for SAR ATR is still in its early stages. And most methods improve upon popular class incremental learning algorithms. Tang et al. [6] combined the three mainstream algorithms mentioned above. The algorithm utilized multimodel knowledge distillation on exemplar set to correct the accumulative errors of old classes, and unstructured pruning initialization to improve the plasticity of model. Li et al. [8] considered that SAR images exhibit significant intraclass differences and small interclass differences due to the fact that targets of the same class at different azimuths have large differences, while targets of different classes at the same azimuth have certain similarities. To address this, the incremental class anchor clustering was proposed to eliminate confusion between old and new classes. In addition, CBesIL [7] and DCBES [9] have emphasized the crucial role of selecting appropriate class exemplars for data-centric methods. CBesIL [7] screens samples from the boundary region using geometric and statistical information. The boundary samples are then used to synthesize samples representing the interior region for new task. Li et al. [9] presented density coverage-based exemplar selection to pick those samples that can cover the class distribution to the maximum extent as exemplars. SSF-IL [32] replaces conventional knowledge distillation with intraclass clustering loss to cluster around the saved class centers, maintaining the separability among the old class features. In addition, some studies have considered incremental SAR ATR under limited samples condition [11], [33]. Zhao et al. [11] proposed cosine prototype learning to resist overfitting on

new classes. Wang et al. [33] further proposed a hybrid distance classifier and pseudoincremental learning strategy to resist forgetting. Although these algorithms achieved good results, they did not consider supplementing the measured data with simulated data under limited samples condition in incremental learning. This motivated our research on the topic.

B. Utilization of SAR Simulated Data

SAR image simulation is a technique used to replicate SAR image features or the SAR system's work process, producing the simulated SAR image. It can be classified into three categories: 1) feature-based; 2) raw signal-based; and 3) SAR image-based [34]. The feature-based approach focuses on the simulation of geometrical and radiometric features of the images, and seeks the similarity between the simulated image and measured images, such as the shape and distribution of scattering points. Given the challenge of acquiring measured data, it is not surprising that numerous methods have been developed to enhance SAR ATR performance by incorporating simulated data into the training set [35], [36], [37].

1) Transfer Learning: One dominant way of utilizing simulated data is through transfer learning [14], [35]. For these methods, the model is pretrained on simulated data and then fine-tuned using a small amount of measured data to learn more useful and generalized features of the simulated data. This enables the model to quickly adapt during retraining with measured data. In addition, some methods extract more generalized feature by domain adaptation. Sun et al. [38] designed a multiscale feature extraction module to extract domain-invariant feature. Further, He et al. [39] proposed a task-drive domain adaptation transfer method to alleviate the degradation of recognition caused by the variance of depression angle between training and test data.

2) Transform and Augment: Some research considers transforming simulated images to be more similar with measured images in image domain. Cha et al. [40] proposed refining simulated data based on deep residual networks. Liu et al. [41] introduced CycleGAN [36] to perform style migration on simulated data. Camus et al. [42] trained a cGAN [43] to refine simulated data by adding MSTAR-specific features. In contrast to simulated image realism, some studies have focused on augmenting the simulated data to improve classifier performance. Song et al. [16] proposed utilizing nonessential factor suppress for preprocess of simulated data. This removes the effect of unimportant textual information from the simulated data. Sellers et al. [44] applied the phase error of measured data to the augment of simulated data. Further, Inkawhich et al. [13] used data augmentation, model construction, loss function choices, and ensembling techniques to enhance the representation learned from the simulated data, and ultimately achieved over 95% accuracy on the SAMPLE dataset.

3) Other Methods: Zhang et al. [37] proposed a multisimilarity fusion (MSF) classifier to comprehensively measure the correlation between the hard samples and the training images. Zhang et al. [15] incorporated SAR domain knowledge related to the azimuth angle, the amplitude, and the phase data of vehicles under few-shot condition. Zhang et al. [45] considers the significance of target scattering features during style migration and modifies the loss function to better retain structural detail information.

In summary, simulated data can effectively assist SAR ATR under small amounts of measured data, few-shot, or zero-shot conditions. This further illustrates the feasibility of applying simulated data to incremental SAR ATR. The simulated data's electromagnetic scattering characteristics benefit both the incremental model's stability and the extraction of new knowledge. However, these methods rarely bridge the gap between simulated and measured data from a class alignment perspective, which is a difficulty that must be overcome by class incremental learning that requires constant processing of unknown data.

III. Proposed Method

In this section, we describe the overall framework of SGFA, as shown in Fig. 3, and explain how to implement incremental recognition with measured and simulated data. Section III-A describes the design of feature aggregation. Section III-B details the incremental learning process.

A. Feature Aggregation

1) Contrastive Loss Design: To extract target-related features that are common to both simulated and measured data, it is necessary to aggregate the distribution of simulated and measured data in the feature space. Metric learning is a useful approach to consider this issue. However, metric learning necessitates the constant construction of positive and negative sample pairs, which increases the complexity of algorithm design. To address this issue, we introduce cyclic shifts, which can automatically construct positive and negative samples in each minibatch [46]. We perform it on feature vectors of minibatch. Specifically, all vectors are shifted back one position, and the final vector is moved to the first position in the minibatch. Assuming that the output vectors of data is $[f1, f2, f3]$, the result of a cyclic shift is $[f3, f1, f2]$. Upon completion of this process, the feature vectors at the designated location constitute an exact sample pair $([(f1, f3), (f2, f1), (f3, f2)])$. Subsequently, the Euclidean distance between samples of the same class is calculated according to the corresponding labels to obtain the contrastive loss by

$$L_{\text{cont}} = \frac{1}{N}\sum_{i=1}^{N} y_i d_i \tag{1}$$

where N denotes the number of feature vectors in the minibatch, d_i denotes the Euclidean distance between the feature vectors at position i in the shift and nonshift feature vectors. If they fall into the same class, y_i is 1, otherwise 0. We solely concentrate on the samples of the same class in the minibatch and minimize their distance in the feature space. We do not introduce negative samples because increasing the distance between classes contradict the feature aggregation between simulated and measured data. Repeat above operations until the first vector is shifted to

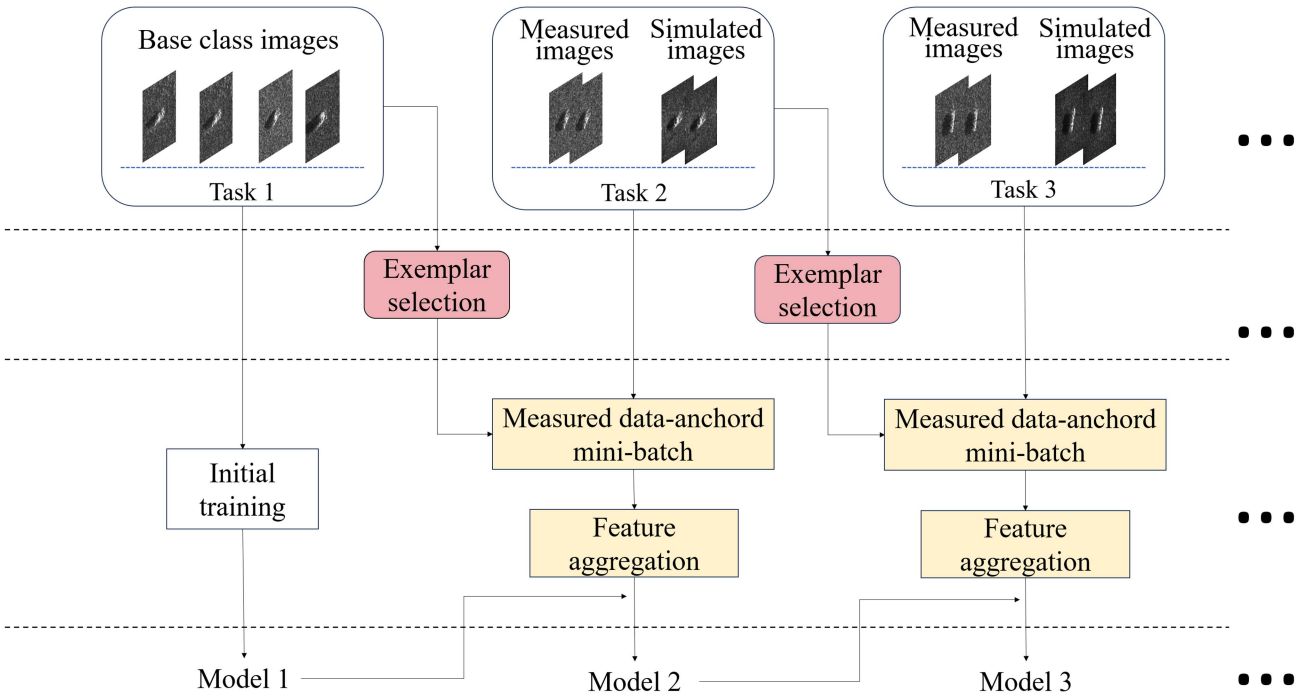

Fig. 3. Framework of SGFA.

Algorithm 1: Compute Contrastive Loss for Minibatch.

Input: $labels, features$
Output: contrastive loss of minibatch
$i \leftarrow 1$
$sum\_loss \leftarrow 0$
$N \leftarrow len(lables)$
$features\_cyc \leftarrow features$
$labels\_cyc \leftarrow labels$
while $i < N$ **do**
$features\_cyc \leftarrow Cyclic(features\_cyc)$
$labels\_cyc \leftarrow Cyclic(labels\_cyc)$
$y \leftarrow labels\_cyc.eq(labels)$
$d \leftarrow ||features\_cyc - features||$
$loss \leftarrow y * d^2$
$sum\_loss \leftarrow loss + sum\_loss$
$i \leftarrow i + 1$
end while
return $sum\_loss/[N * (N-1)]$

the last and then calculate the final loss by

$$L = L_c + \frac{\lambda}{N-1} \sum_{j=1}^{N-1} L_{\text{cont}}^{j} \tag{2}$$

where L_c denotes the cross entropy loss, L_{cont}^{j} denotes contrastive loss of jth cycle shift, λ is a hyperparameter. Algorithm 1 shows the detailed processing flow.

2) Measured Data-Anchored Minibatch: The amount of simulated data per class is much larger than the measured data, making it difficult for the measured data to participate in each minibatch build. The direct feature aggregation of minibatches constructed by random sampling is more about clustering simulated data than aggregating feature distribution of simulated and measured data. Hence, we propose a MDA. Specially, we add all the measured data and randomly selected simulated data to each minibatch, which is for the effective feature aggregation. In addition, we found that aggregating features only for the new classes of simulated and measured data causes the model to overlook the separability of the new classes from the old ones. This leads to unsatisfactory recognition of new classes. Hence, a portion of exemplars is added to the minibatch to maintain the separability of the different classes. The specific operation is shown in Fig. 5. Separate minibatch streams are created for the simulated data and the exemplar set. These two streams output minibatches one-by-one, which are then concatenated to the measured data to construct a training minibatch.

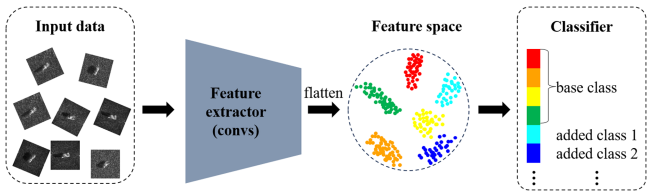

Fig. 4. Schematic diagram of network structure.

B. Incremental Learning

1) Data Format: For typical class incremental leaning, it aims to learn from a data stream with incoming new classes. The data stream can be divided into a sequence of recognition tasks $\{T_1, T_2, \ldots, T_n\}$, and $\{D_1, D_2, \ldots, D_n\}$ are the corresponding

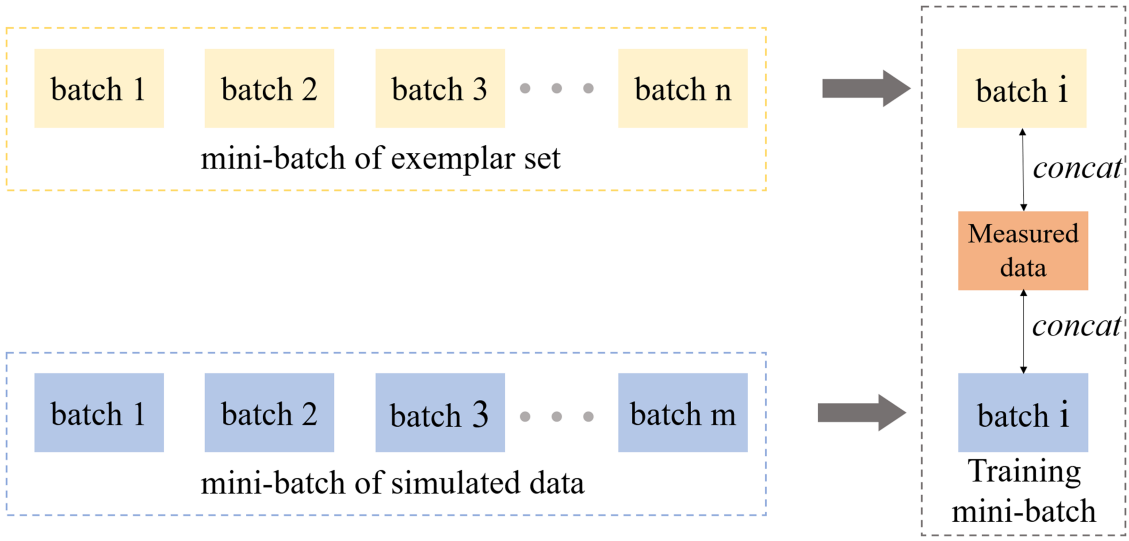

Fig. 5. Illustration of measured data-anchored minibatch construction. The blue rectangles and yellow rectangles represent the minibatch of the simulated data and the exemplar set, respectively, which are concatenated with the measured data (orange rectangle) in parallel to form the training minibatch.

labeled training set, with $D_n = (x_i, y_i), i \leq N_b$, where x_i is image sample, $y_i \in C_n$, N_b is the number of training samples in D_n, and C_n is the label space of D_n, the label spaces of different tasks do not overlap. In each incremental task, the model processes the current data while accessing or failing to access only a small portion of the past data, and at the end of the task, the model has to maintain its ability to discriminate the old classes while learning discriminative knowledge about the new ones. In this article, D_1, as base class data, only includes measured images. The follow-up data $(D_2, D_3, \ldots, D_n)$ consists of limited measured images and an adequate number of simulated images of new classes.

2) Network Architecture: As a foundation support, our method makes use of convolutional neural network. We think of the network a trainable feature extractor followed by a classifier which has as many output nodes as classes observed so far. The network in our method is ResNet18, with the last linear layer as classifier $f(\cdot)$ and the other layers as feature extractor $\phi(\cdot)$. As shown in Fig. 4, the input image is fed into the network, and the output of the final convolutional layer is flattened to obtain the feature vector, which is subsequently fed into the linear layer to get the prediction. Since our method is not limited to specific network structures, it can be replaced with other CNN networks.

3) Initial Learning: As shown in Fig. 3, in the initial learning phase, a model is trained directly using the cross entropy loss, since the base class data is all measured data. After initial training session, all of the data is once again fed back into the feature extractor to get the feature vectors. Further, we compute prototypes for each class in preparation for subsequent exemplar set construction. The prototype can be calculated by

$$p_y = \frac{1}{|D_y|} \sum_{x \in D_y} \phi(x) \tag{3}$$

where D_y is the training data of class y. Then, exemplars for each class are selected by herding, which makes the center of the feature vectors of the samples in the exemplar set closest to which of the entire training set. The operation is shown as below

$$e_k = \arg\min_{x \in D_y} \left|\left| p_y - \frac{1}{k} \left[\phi(x) + \sum_{i=1}^{k-1} \phi(e_i) \right] \right|\right|, k = 1, 2, \cdots, q \tag{4}$$

where e_k is the kth selected exemplar for class y and q is the number of exemplars for each class.

4) Learning From New Tasks: In the incremental learning phase, exemplar set are included in model training in addition to the new classes of measured and simulated data. Initially, the training minibatch is conducted by measured data-anchored minibatch construction strategy. Then it is delivered to the feature extractor to acquire feature vectors. The feature vectors are fed into the classifier to calculate the cross entropy loss. Naturally, the output nodes of the classifier increase to the same number of known classes. Specifically, when new classes of data are introduced, a new classifier is instantiated whose number of output nodes is the sum of the number of new classes and the number of existing classes. Subsequently, the parameters of the previous classifier are allocated to the corresponding nodes of the new classifier, with no operations being conducted on the new nodes. This process preserves to some extent the knowledge of the previous classes.

For feature aggregation, cyclic shifts are performed on these feature vectors of minibatch to compute contrastive loss. The contrastive loss and cross entropy loss synchronized to model update. After training, similarly we select samples to be added to the exemplar set. However, since the limited measured samples of new class make the model susceptible to overfitting, even retaining all measured data as exemplars was difficult to sustain the model's ability to recognize this target in subsequent incremental tasks, resulting in dramatic forgetting of the model's knowledge about it. With this in mind, a small amount of simulated data is added to the exemplar set to resist forgetting. For the selection of simulated data, we hope to select which is closer to the measured

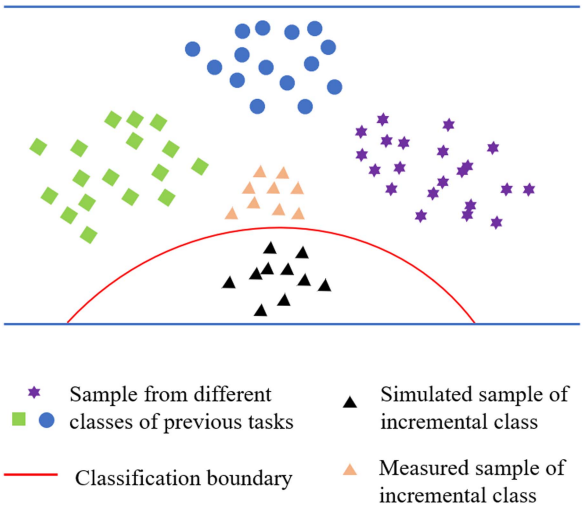

Fig. 6. Schematic of classification results for strong classification boundaries.

data. Inspired by herding, we utilize the mean of the feature vectors of the measured data instead of the center of the entire training set to select the simulated data. Details of incremental training step is shown in Algorithm 2. Subsequent incremental tasks are carried out according to the above flow path.

5) Classification: At the test stage, although the classifier can directly predict the probability of classes, the strong classification boundaries of classifier will cause misjudgment of the classes of measured data when there is a certain distance between the measured data and simulated data in the feature space, as shown in Fig. 6. Hence, we use it only for representation learning. For classification, we rely on exemplar set to establish a prototype for each class. The prototype can be calculated by

$$p_y = \frac{1}{|M_y|} \sum_{m \in M_y} \phi(m) \tag{5}$$

where M_y is the exemplar set of class y. For a image x should be classified, assuming the space of classes observed so far is C_O, we assign the class label of the most similar prototype to it

$$y^* = \arg\min_{y \in C_o} ||\phi(x) - p_y||. \tag{6}$$

IV. Experimental Evaluation

In this section, experiments are carried out to evaluate the effectiveness of the proposed method. We use publicly available subset of the Synthetic and Measured Paired Labeled Experiment (SAMPLE) for experimental evaluation.

A. Dataset and Experimental Setup

1) Dataset: The SAMPLE dataset, supported by air force research laboratory (AFRL), consists of measured SAR images from the MSTAR data collect and is paired with simulated SAR images of ten classes of military vehicles, i.e., 2S1, BMP2, BTR70, M1, M2, M35, M60, M548, T72, ZSU23-4. The measured images and simulated images of ten classes in the SAMPLE dataset are shown in Fig. 7. The publicly available

Algorithm 2: Incremental Training.

Input: $X_m, X_s, M, \phi^{t-1}, f^{t-1}$ // measured data, simulated data, exemplar set, feature extractor and classifier of previous task

Output: ϕ^t, f^t // feature extractor and classifier of current task

$\phi^t \leftarrow \phi^{t-1}$

$f^t \leftarrow f^{t-1} + o_c$ // add output nodes

for $i < N$ **do**

$b \leftarrow MDA(X_m, X_s, M)$

$feature \leftarrow \phi^t(b)$

$L_{cont} \leftarrow$ Compute contrastive loss by $feature$

$logits \leftarrow f^t(feature)$

$L_C \leftarrow$ Compute cross entropy loss by $logits$

$L \leftarrow L_C + \lambda * L_{cont}$

Update ϕ^t, f^t by L

end for

TABLE I
Experimental Setup of SAMPLE Dataset

class	Train		Test
	measured	simulated	measured
2S1	35	0	139
BMP2	22	0	85
BTR70	18	0	74
M1	26	0	103
M2	3	128	125
M35	3	129	126
M60	3	176	173
M548	3	128	125
T72	3	108	105
ZSU23-4	3	174	171

SAMPLE data are sampled in azimuth from 10° to 80° and in elevation from 14° to 17°. The measured data was divided into training set and test set in a 1:4 ratio for base classes (2S1, BMP2, BTR70, M1). As to incremental classes, the training set comprises all simulated images and three randomly selected measured images, and the remaining measured images constitute the test set. Detailed information is listed in Table I. The original image size is 128×128. To reduce the impact of background clutter, the images are cropped to 88×88.

There are three incremental experimental scenarios, where the number of newly added classes is 1, 2, and 3 each time and the number of base classes is 4. The tasks for each scenario are divided as shown in Table II.

2) Evaluation Metrics: The average recognition accuracy of all known classes for each incremental task can be used as one of the evaluation indicators, which reflects the overall performance of the algorithm. However, the stability and plasticity which is the main focus of performance in incremental learning of these methods cannot be reflected in average accuracy. Therefore, the accuracy of each class per incremental task can be one of the

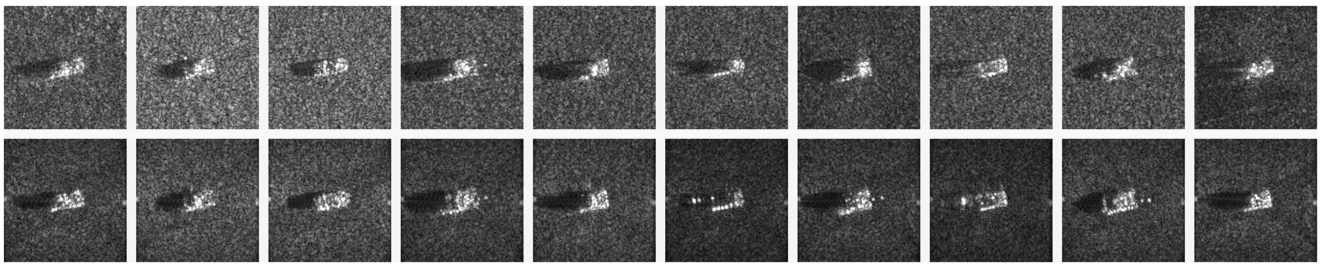

Fig. 7. Measured images (Top) and simulated images (Bottom) of SAMPLE dataset. The class order is: 2S1, BMP2, BTR70, M1, M2, M35, M60, M548, T72, ZSU23-4.

TABLE II
INCREMENTAL EXPERIMENTAL SCENARIOS

Scenario	2S1	BMP2	BTR70	M1	M2	M35	M60	M548	T72	ZSU23-4
Scenario 1	TASK 1				TASK 2	TASK 3	TASK 4	TASK 5	TASK 6	TASK 7
Scenario 2	TASK 1				TASK 2		TASK 3		TASK 4	
Scenario 3	TASK 1				TASK 2			TASK 3		

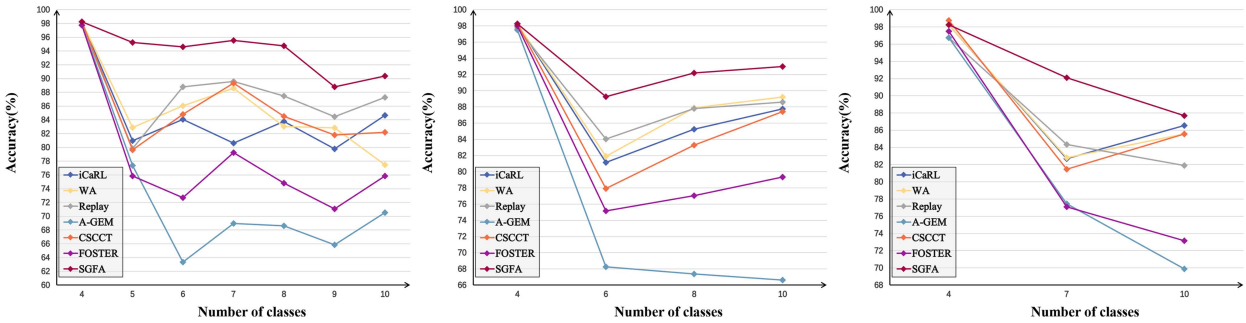

Fig. 8. Incremental recognition accuracies of scenario 1 (Left), 2 (Middle), and 3 (Right).

metrics. In addition, to verify whether the algorithm can extract common features between simulated and measured data, t-SNE is given to be a considerable metrics.

3) Implementation Details: All experiments are performed on PyTorch framework, which use a personal computer with NVIDIA RTX 3090 on Windows 10 system. In our method, each training phase contains 1000 batches for initial learning and incremental learning. The minibatch size is 20 for scenarios 1, 2, and 30 for scenario 3. In the incremental learning, each minibatch contains measured data for all the newly added classes, and an equal number of simulated data, with the remainder being exemplars. Specifically, the number of simulated and measured data for each category is both 3, and the number of exemplars is 14, 8 and 12 for scenarios 1, 2, and 3. The number of exemplars per class is 15, with the base classes consisting of measured images and the incremental classes consisting of three measured images and 12 simulated images. The stochastic gradient descent is applied as an optimizer, where the learning rate is 0.001 and the momentum factor is 0.9. The hyperparameter $\lambda = 0.5$.

B. Incremental Recognition Performance

In this section, experiments are conducted in different incremental conditions to validate the effectiveness of our approach. Since SGFA belongs to data-centric method, we mainly compared it with prior data-centric methods—iCaRL [4], WA [5], A-GEM [23], FOSTER [30], CSCCT [31]. Furthermore, to verify the validity of the feature aggregation, a baseline Replay was also added to the comparison, which was trained purely using the exemplars and new data without any other manipulations.

1) Performance Under Different Scenarios: Fig. 8 illustrates the average accuracy of the above method after each incremental task in the three experimental scenarios. As seen in Fig. 8, our method achieves the best recognition accuracy in all incremental tasks. iCaRL, WA, Replay, and CSCCT based on direct training of the replay data perform similarly in different incremental scenarios. Although FOSTER has devised a more intricate learning methodology to address the issue of forgetting, the intricate algorithmic design is inadequate in the context of the complex data distribution, resulting in suboptimal outcomes. Since these methods do not account for the distributional differences between simulated and measured data, the overall recognition results are unsatisfactory and unstable. It can be seen that a dramatic drop in recognition rate occurs at the first incremental task in all scenarios. This phenomenon occurs because, when simulated data is initially added for training, the model tends to extract simulated-specific to separate new and old classes due to the large amount of simulated data in the new class

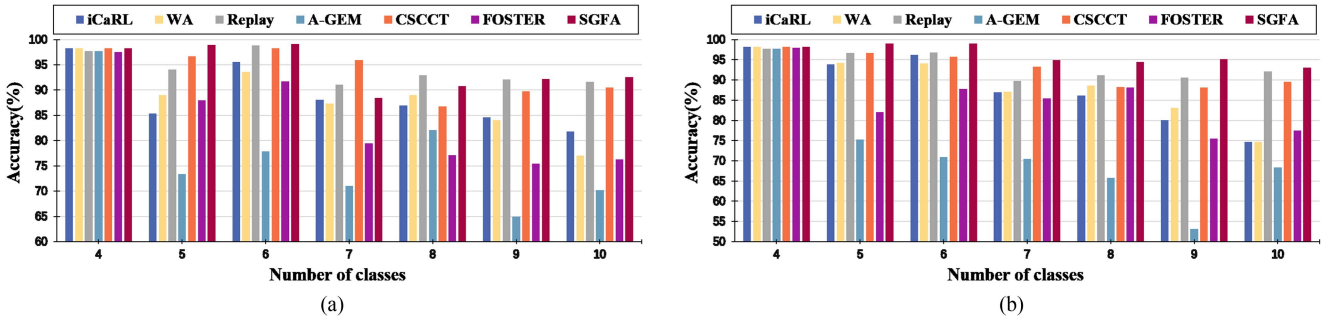

Fig. 9. Incremental recognition accuracies under different incremental class order, where the number of incremental classes is 1 for each task. (a) The order is M60, M548, T72, ZSU23-4, M2, M35. (b) The order is T72, ZSU23-4, M2, M35, M60, M548.

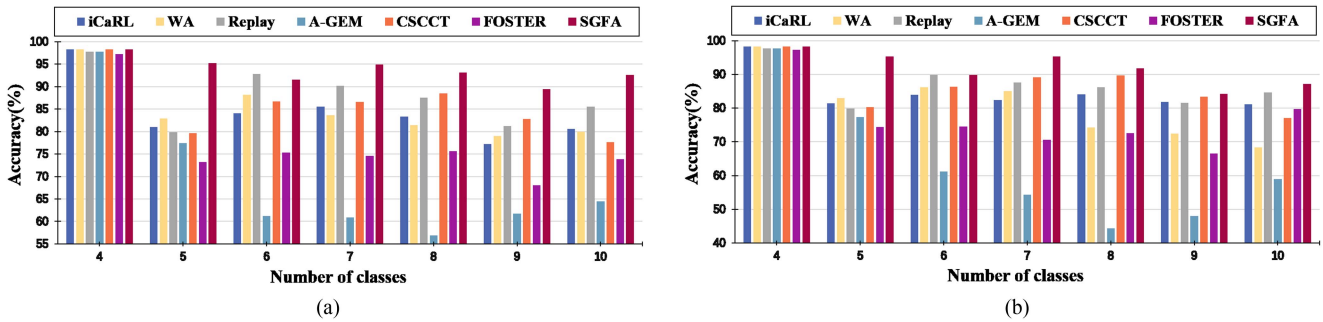

Fig. 10. Incremental recognition accuracies of scenario 1 under different number of simulated exemplar (E_s). (a) $E_s = 7$. (b) $E_s = 2$.

compared to the measured data in the base class. In addition, the proximity of M2 and BMP2 in the feature space is notable. The distance even smaller than that between simulated and measured data, leading to misclassification. This can be further verified in the subsequent visualization results. This similarity may be attributed to shared structures, such as high hulls, short gun barrels, and tracks. Instead, SGFA extracts fine structural features through feature aggregation, improving the separability of M2. A-GEM, on the other hand, uses the exemplar set to standardize the direction of model gradient updating, which rely on the accuracy of its assumptions. In the presence of a complex distribution of new class data, significant forgetting occurred, leading to poor overall performance.

In addition, in scenario 3, the model's performance declines rapidly in the final task. This is due to the fact that SGFA primarily focuses on the learning of new classes, with minimal attention paid to the problem of forgetting old classes containing simulated exemplars. In contrast, in scenario 3, the maximum number of new classes is added in each task, leading the model to prioritize the new classes, which exacerbates the forgetting process.

2) Performance Under Different Incremental Conditions: Fig. 9 illustrates the experimental results for different incremental classes order conditions in scenario 1. It can be found that under two different incremental classes orders, SGFA achieved the highest recognition accuracy at the end of the final task. As shown in Fig. 9, there is some degradation in performance when processing simulated data for the first time. However, the degree of degradation varies. As described in the analysis of Fig. 8, the recognition accuracy is affected by the similarity between new and old classes, which causes this phenomenon. The SGFA effectively reduces the distribution of simulated and measured data in the feature space and is less affected by it. Therefore, this abrupt change did not occur in both conditions.

For data-centric methods, the number of exemplars has a significant impact on the performance of the algorithm. Thus, experiments were conducted under various exemplar set size (only for simulated exemplars) conditions. As shown in Fig. 10, although SGFA's performance decreases with fewer simulated examples, it still outperforms other methods overall. It is important to note that, even with varying numbers of simulated exemplars and different orders of incremental classes, the recognition performance after processing the final class of data is second only to SGFA and even exceeds it in some tasks. This suggests that specific incremental algorithms may not be helpful when introducing simulated data.

3) Recognition Accuracy per Class at Each Task: Table III exhibits the recognition accuracy per class at the end of each incremental task of iCaRL, WA, Replay, SGFA in scenario 1. It can be seen that the recognition accuracy of the base classes is not much affected as new data is continuously processed in SGFA, Replay, iCaRL, and WA (except for last task). This is mainly because the SAMPLE dataset only includes a portion of the azimuthal samples. Therefore, a small number of exemplars can effectively characterize the class features. In addition, at the end of each incremental training, SGFA achieves the highest recognition accuracy for newly added classes. Other methods are less effective without aggregating the feature distribution of the simulated and measured data. After the first incremental task, SGFA's recognition performance for M2 is 58.4%, 52%, and

TABLE III
RECOGNITION ACCURACY PER CLASS OF ICARL, WA, REPLAY, SGFA IN SCENARIO 1(%)

TASK	iCaRL										WA									
	2S1	BMP2	BTR70	M1	M2	M35	M60	M548	T72	ZSU23-4	2S1	BMP2	BTR70	M1	M2	M35	M60	M548	T72	ZSU23-4
T_1	97.12	97.65	98.65	100	-	-	-	-	-	-	96.40	98.82	98.65	100	-	-	-	-	-	-
T_2	94.24	100	100	100	26.40	-	-	-	-	-	94.40	98.82	100	100	32.80	-	-	-	-	-
T_3	95.53	100	100	100	43.20	80.95	-	-	-	-	96.40	98.82	100	99.03	48.80	84.13	-	-	-	-
T_4	95.68	100	98.65	100	35.20	**92.06**	64.16	-	-	-	94.40	100	100	99.03	**49.60**	**89.68**	**93.06**	-	-	-
T_5	94.69	98.82	100	100	**57.60**	39.68	90.75	**99.20**	-	-	96.40	100	100	99.03	40.80	49.21	90.75	**99.20**	-	-
T_6	94.96	97.65	95.95	99.03	42.40	30.95	83.24	99.20	89.52	-	92.09	97.65	98.65	98.06	41.60	53.97	86.71	92.8	**98.1**	-
T_7	93.53	95.29	100	99.03	28.00	50.79	**98.84**	95.20	**91.43**	**97.08**	78.42	80.00	86.49	97.09	20.00	58.73	83.82	85.60	87.62	**97.08**
	Replay										SGFA									
T_1	97.12	96.47	97.30	100	-	-	-	-	-	-	97.12	97.65	98.65	100	-	-	-	-	-	-
T_2	95.68	98.82	100	100	20.80	-	-	-	-	-	95.68	100	100	100	**84.80**	-	-	-	-	-
T_3	95.68	98.82	100	100	**55.20**	92.06	-	-	-	-	95.68	100	100	100	80.00	**96.83**	-	-	-	-
T_4	96.40	98.82	100	100	44.00	**93.65**	**98.84**	-	-	-	96.40	100	100	100	79.20	95.24	**100**	-	-	-
T_5	96.40	98.82	100	100	38.40	73.81	**98.84**	99.20	-	-	96.40	100	100	100	84.00	80.16	**100**	**100**	-	-
T_6	96.40	98.82	100	100	41.60	57.14	82.66	**100**	**100**	-	95.68	100	100	100	64.80	73.81	79.77	**100**	**100**	-
T_7	96.40	98.82	100	100	36.00	65.08	90.17	**100**	**100**	**94.74**	95.68	98.82	100	100	52.80	79.37	88.44	99.20	**100**	**97.08**

Bolded numbers indicate the highest recognition accuracy for incremental class across all incremental tasks.

64% higher than that of iCaRL, WA, and Replay, respectively. In general, the model performs best at recognizing the added data when it first occurs. However, the simulated data have introduced bias, leading to different results in iCaRL, WA, and Replay. For example, as shown in Table III, the recognition accuracy of M2, M35, M60 at first processing is lower than that of follow-up task. In contrast, SGFA performs at its best when it initially learns classes using simulated data. This further illustrates the ability of SGFA to mitigate the effects of biased knowledge of simulated data.

4) Visualization Results: Fig. 11 shows the t-SNE results of the simulated and measured data after each incremental task in scenario 1. Four phenomena can be found in Fig. 11. First, in SGFA, the distribution difference between simulated and measured data is significantly reduced compared to other methods. Second, there is still a tendency for the feature distributions of the simulated and measured data of the old classes to converge when dealing with the new data. However, other methods do not have this effect, such as M35 from task 4 to task 6. This is because exemplars are being added to the training minibatch for feature aggregation. Third, although there are differences in the feature distributions of the measured and simulated data for M2 among the four methods in task 2, SGFA effectively suppresses confusion by increasing the class spacing between the new class and the base class through feature aggregation. As a result, the recognition accuracy of M2 is significantly higher in task 2 compared to the other three methods. Finally, the distribution of features in aggregated simulated and measured data also has a clustering effect. For example, although Replay does not suffer from base class confusion in WA and iCaRL, however, the distribution of feature points of the same class in Replay is significantly more spread out, which is more concentrated in SGFA.

C. Ablation Experiment

1) Effectiveness of Different Components: In order to analyze the impact of each component of the proposed method, the experimental results for each scenario with different components are presented in Table IV. Herd denotes the herding selection method. It can be observed that in the preincremental task, which is the initial introduction of the simulated data, MDA and L_{cont} demonstrate a notable enhancement in the performance of the model. Conversely, Herd exhibits enhanced stability in the subsequent incremental tasks as the number of categories increases. Ultimately, the highest average recognition accuracies are achieved in both scenario 1 and scenario 2 with the integration of all three. Although the optimal outcomes were not attained in scenario 3 under the role of the three components, it is evident that these three components play a more pronounced role in the incremental tasks at different stages (highest accuracy rate in task 2 with MDA and L_{cont}, highest accuracy rate in task 3 with only Herd).

2) Influence of the Number of Simulated Exemplars: To further validate the effectiveness of adding simulated data to the exemplar set, we conduct experiments under different exemplar set size in three scenarios. Table V shows the recognition accuracy under different number of simulated exemplars ($E_s = 0, 2, 7, 12$ per class only for simulated data). It can be seen that the model's recognition performance is not greatly affected for short-term incremental tasks. However, with the addition of new classes, the model recognition accuracy drops dramatically in the smaller settings of the exemplar set. At the end of the last incremental task, SGFA-0 was 11.59%, 9.30%, 10.11% lower than SGFA-12 in the three scenarios, respectively. This difficulty arises from the challenge of accurately representing the old classes distributions with a limited number of exemplars. As a result, the incremental

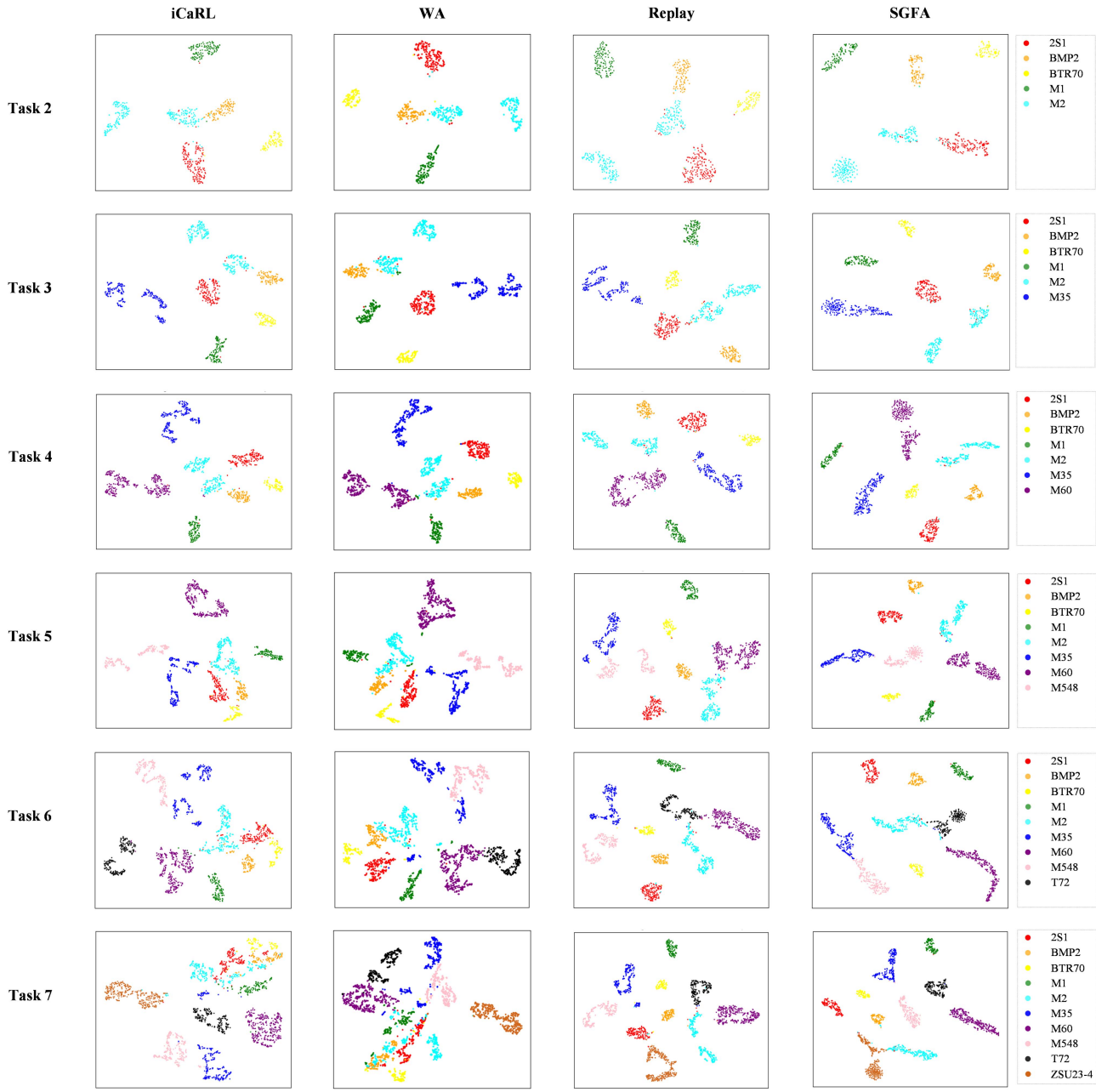

Fig. 11. t-SNE results of iCaRL, WA, Replay, SGFA in scenario 1.

TABLE IV
EXPERIMENTAL RESULTS FOR DIFFERENT COMBINATIONS OF COMPONENTS IN THREE INCREMENTAL SCENARIOS(%)

MDA	L_{cont}	Herd	Scenario 1								Scenario 2					Scenario 3			
			T_1	T_2	T_3	T_4	T_5	T_6	T_7	AA	T_1	T_2	T_3	T_4	AA	T_1	T_2	T_3	AA
✓			98.25	89.73	92.94	92.48	91.37	**91.00**	89.48	92.18	98.25	90.34	92.84	90.70	93.03	98.25	88.48	85.32	90.68
	✓		98.25	92.59	90.34	91.88	93.16	86.82	89.31	91.76	98.25	**91.41**	91.05	87.44	92.04	98.25	93.33	87.44	93.01
		✓	98.25	81.94	90.80	93.58	92.32	90.14	**90.54**	91.08	98.25	83.13	88.84	90.62	90.21	98.25	86.18	**90.62**	91.68
✓	✓		98.25	**95.25**	93.87	93.45	91.05	85.88	85.40	91.88	98.25	88.80	90.53	87.19	91.19	98.25	**95.03**	86.95	**93.41**
✓		✓	98.25	88.59	88.80	89.70	86.42	84.17	86.70	88.95	98.25	88.50	91.26	89.56	91.89	98.25	87.39	84.42	90.02
	✓	✓	98.25	87.45	86.81	88.24	83.79	81.04	78.47	86.29	98.25	87.27	**93.37**	92.58	92.87	98.25	90.79	88.09	92.38
✓	✓	✓	98.25	**95.25**	**94.63**	**95.52**	**94.74**	88.82	90.38	**93.94**	98.25	89.26	92.21	**92.99**	**93.18**	98.25	92.12	87.68	92.68

Bolded numbers indicate optimal results.

TABLE V
EXPERIMENTAL RESULTS FOR DIFFERENT NUMBER OF SIMULATED EXEMPLARS IN THREE INCREMENTAL SCENARIOS(%)

E_s	Scenario 1								Scenario 2					Scenario 3			
	T_1	T_2	T_3	T_4	T_5	T_6	T_7	AA	T_1	T_2	T_3	T_4	AA	T_1	T_2	T_3	AA
0	98.25	95.25	89.57	93.94	88.53	76.49	78.79	88.69	98.25	89.26	86.00	83.69	89.30	98.25	92.12	77.57	89.31
2	98.25	95.25	89.88	95.27	91.79	84.27	87.11	91.69	98.25	89.26	90.32	84.50	90.58	98.25	92.00	82.54	90.93
7	98.25	95.25	91.56	94.91	93.16	89.38	**92.58**	93.58	98.25	89.26	90.11	87.85	91.37	98.25	92.00	87.6	92.62
12	98.25	95.25	94.63	95.52	94.74	88.82	90.38	**93.94**	98.25	89.26	92.21	**92.99**	**93.18**	98.25	92.12	**87.68**	**92.68**

Bolded numbers indicate optimal results, the red numbers indicate the recognition accuracy for the task 2.

TABLE VI
RECOGNITION ACCURACY PER CLASS OF SGFA-0 IN SCENARIO 1(%)

Task	2S1	BMP2	BTR70	M1	M2	M35	M60	M548	T72	ZSU23-4
T_1	97.12	97.65	98.65	100	-	-	-	-	-	-
T_2	95.68	100	100	100	84.80 (-)	-	-	-	-	-
T_3	95.68	100	100	100	53.60 (26.40↓)	96.83 (-)	-	-	-	-
T_4	94.96	100	100	100	69.60 (9.60↓)	96.03 (0.79↑)	100 (-)	-	-	-
T_5	96.40	100	100	100	72.00 (12.00↓)	45.24 (34.92↓)	100 (-)	100 (-)	-	-
T_6	95.68	100	100	100	54.40 (10.40↓)	45.24 (28.57↓)	32.37 (47.40↓)	100 (-)	100 (-)	-
T_7	92.81	100	100	100	32.80 (20.00↓)	47.62 (31.75↓)	43.35 (45.09↓)	100 (0.80↑)	99.05 (0.95↓)	99.42 (2.34↑)

Parenthesis content is the difference in recognition accuracy between SGFA-0 and SGFA-12, with ↑ denoting higher, ↓ denoting lower than SGFA-12 and (-) denoting equal.

TABLE VII
EXPERIMENTAL RESULTS FOR VARIOUS VALUES OF λ IN THREE INCREMENTAL SCENARIOS(%)

λ	Scenario 1		Scenario 2		Scenario 3	
	T_7	AA	T_4	AA	T_3	AA
0.0	86.70	88.95	89.56	91.56	84.42	90.02
0.1	88.91	91.41	91.19	92.90	84.42	90.87
0.2	88.25	92.62	90.54	**93.33**	83.52	90.69
0.3	89.40	92.78	89.56	92.22	86.22	91.95
0.4	85.97	93.24	92.33	93.25	87.28	92.23
0.5	90.38	**93.94**	**92.99**	93.18	87.68	92.68
0.6	89.97	93.34	92.21	93.16	90.13	94.07
0.7	89.31	92.19	89.31	90.85	88.99	93.32
0.8	91.84	92.52	90.46	92.33	88.25	93.36
0.9	91.19	91.79	91.52	91.94	88.09	92.78
1.0	**92.41**	92.30	91.84	92.66	**90.29**	**94.08**

Bolded numbers indicate optimal results.

classes, which only has three measured images as exemplars, is particularly susceptible to forgetting.

As shown in Table VI, the learning ability for new classes is essentially the same for both SGFA-12 and SGFA-0, but the accuracy of recognizing incremental classes that retain only measured exemplars declines rapidly when subsequent data arrives. In addition, the model's performance in task 2 (red value in Table V) remains consistent across various exemplar set sizes in all scenarios. There are two reasons for this. First, SGFA can effectively bring the feature distributions of simulated and measured data closer together. Second, the herding-based exemplar selection method can select simulated samples closer to the feature centers of the measured samples. This ensures that the class prototype are not affected too much by the introduction of simulated exemplars.

3) Influence of λ: In order to study the effect of λ on the performance of incremental recognition, we assign λ values from 0 to 1 at 0.1 intervals. $\lambda = 0$ means that no computation of contrastive loss is performed and only a measured data-anchored minibatch is constructed. Finally, we get the results as shown in Table VII. From the table, it can be seen that the accuracy of the recognition can be significantly improved even if the λ is set to a relatively small value. Although model can learn from newly added data effectively with feature aggregation operation, the issue of degraded recognition performance for old classes that contain simulated data is not been adequately addressed. Therefore, as the value of λ increases from 0.6 to 1, there is no significant improvement in overall recognition accuracy.

V. CONCLUSION

In this article, simulated data is introduced into class incremental learning to address the issue of limited new target samples in open scenario. We found that incremental models tend to favor simulated-specific feature learning to differentiate simulated data of new classes from measured exemplars of old classes. This hinders the effective extraction of knowledge about new classes. To tackle this problem, a novel method SGFA for incremental SAR ATR is proposed. In each minibatch, SGFA aggregates the feature distributions of both simulated and measured data of same class through cyclic shifts, with the aim of guiding the model in learning the target-related features. Then, a small amount of simulated data is retained as exemplars to resist catastrophic forgetting. The experiment on the SAMPLE dataset shows that SGFA outperforms mainstream data-centric incremental learning methods. The visualization results of simulated and measured data further demonstrate that it can effectively eliminate the distribution discrepancy of them. However, the recognition accuracy of classes containing simulated exemplars

decreases more severely compared to base classes with the addition of new classes. This could be a result of inadequate utilization of the simulated exemplars. The authors will try to address this issue in future work.

REFERENCES

[1] A. Moreira, P. Prats-Iraola, M. Younis, G. Krieger, I. Hajnsek, and K. P. Papathanassiou, "A tutorial on synthetic aperture radar," *IEEE Geosc. Remote Sens. Mag.*, vol. 1, no. 1, pp. 6–43, Mar. 2013.

[2] S. Chen, H. Wang, F. Xu, and Y.-Q. Jin, "Target classification using the deep convolutional networks for SAR images," *IEEE Trans. Geosci. Remote Sens.*, vol. 54, no. 8, pp. 4806–4817, Aug. 2016.

[3] H. Anas, H. Majdoulayne, A. Chaimae, and S. M. Nabil, "Deep learning for SAR image classification," in *Intell. Syst. Appl.: Proc. Intell. Syst. Conf.*, 2020, vol. 1, pp. 890–898.

[4] S.-A. Rebuffi, A. Kolesnikov, G. Sperl, and C. H. Lampert, "iCaRL: Incremental classifier and representation learning," in *Proc. IEEE Conf. Comput. Vis. Pattern Recognit.*, 2017, pp. 2001–2010.

[5] B. Zhao, X. Xiao, G. Gan, B. Zhang, and S.-T. Xia, "Maintaining discrimination and fairness in class incremental learning," in *Proc. IEEE/CVF Conf. Comput. Vis. Pattern Recognit.*, 2020, pp. 13208–13217.

[6] J. Tang, D. Xiang, F. Zhang, F. Ma, Y. Zhou, and H. Li, "Incremental SAR automatic target recognition with error correction and high plasticity," *IEEE J. Sel. Topics Appl. Earth Observ. Remote Sens.*, vol. 15, pp. 1327–1339, 2022.

[7] S. Dang, Z. Cao, Z. Cui, Y. Pi, and N. Liu, "Class boundary exemplar selection based incremental learning for automatic target recognition," *IEEE Trans. Geosci. Remote Sens.*, vol. 58, no. 8, pp. 5782–5792, Aug. 2020.

[8] B. Li, Z. Cui, Z. Cao, and J. Yang, "Incremental learning based on anchored class centers for SAR automatic target recognition," *IEEE Trans. Geosci. Remote Sens.*, vol. 60, 2022, Art. no. 5235313.

[9] B. Li, Z. Cui, Y. Sun, J. Yang, and Z. Cao, "Density coverage-based exemplar selection for incremental SAR automatic target recognition," *IEEE Trans. Geosci. Remote Sens.*, vol. 61, 2023, Art. no. 5211713.

[10] B. Lewis, T. Scarnati, E. Sudkamp, J. Nehrbass, S. Rosencrantz, and E. Zelnio, "A SAR dataset for ATR development: The synthetic and measured paired labeled experiment (sample)," *Proc. SPIE*, vol. 10987, pp. 39–54, 2019.

[11] Y. Zhao, L. Zhao, D. Ding, D. Hu, G. Kuang, and L. Liu, "Few-shot class-incremental SAR target recognition via cosine prototype learning," *IEEE Trans. Geosci. Remote Sens.*, vol. 16, 2023, Art. no. 5212718.

[12] C. Tian, Z. Zhang, X. Gao, H. Zhou, R. Ran, and Z. Jiao, "An implicit-explicit prototypical alignment framework for semi-supervised medical image segmentation," *IEEE J. Biomed. Health Informat.*, vol. 28, no. 2, pp. 929–940, Feb. 2024.

[13] N. Inkawhich et al., "Bridging a gap in SAR-ATR: Training on fully synthetic and testing on measured data," *IEEE J. Sel. Topics Appl. Earth Observ. Remote Sens.*, vol. 14, pp. 2942–2955, 2021.

[14] D. Malmgren-Hansen, A. Kusk, J. Dall, A. A. Nielsen, R. Engholm, and H. Skriver, "Improving SAR automatic target recognition models with transfer learning from simulated data," *IEEE Geosci. remote Sens. Lett.*, vol. 14, no. 9, pp. 1484–1488, Sep. 2017.

[15] L. Zhang et al., "Domain knowledge powered two-stream deep network for few-shot SAR vehicle recognition," *IEEE Trans. Geosci. Remote Sens.*, vol. 60, 2022, Art. no. 521531.

[16] Q. Song, H. Chen, F. Xu, and T. J. Cui, "EM simulation-aided zero-shot learning for SAR automatic target recognition," *IEEE Geosci. Remote Sens. Lett.*, vol. 17, no. 6, pp. 1092–1096, Jun. 2020.

[17] D.-W. Zhou, Q.-W. Wang, Z.-H. Qi, H.-J. Ye, D.-C. Zhan, and Z. Liu, "Deep class-incremental learning: A survey," 2023, *arXiv:2302.03648*.

[18] D. Isele and A. Cosgun, "Selective experience replay for lifelong learning," in *Proc. AAAI Conf. Artif. Intell.*, 2018, vol. 32, no. 1, pp. 1–8.

[19] D. Rolnick, A. Ahuja, J. Schwarz, T. Lillicrap, and G. Wayne, "Experience replay for continual learning," *Adv. Neural Inf. Process. Syst.*, vol. 32, pp. 1–11, 2019.

[20] L. Wang, K. Yang, C. Li, L. Hong, Z. Li, and J. Zhu, "Ordisco: Effective and efficient usage of incremental unlabeled data for semi-supervised continual learning," in *Proc. IEEE/CVF Conf. Comput. Vis. Pattern Recognit.*, 2021, pp. 5383–5392.

[21] W. Sun, Q. Li, J. Zhang, D. Wang, W. Wang, and Y.-a. Geng, "Exemplar-free class incremental learning via discriminative and comparable parallel one-class classifiers," *Pattern Recognit.*, vol. 140, 2023, Art. no. 109561.

[22] D. Lopez-Paz and M. Ranzato, "Gradient episodic memory for continual learning," *Adv. Neural Inf. Process. Syst.*, vol. 30, pp. 1–10, 2017.

[23] A. Chaudhry, M. Ranzato, M. Rohrbach, and M. Elhoseiny, "Efficient lifelong learning with a-gem," 2018, *arXiv:1812.00420*.

[24] J. Kirkpatrick et al., "Overcoming catastrophic forgetting in neural networks," *Proc. Nat. Acad. Sci.*, vol. 114, no. 13, pp. 3521–3526, 2017.

[25] A. Chaudhry, P. K. Dokania, T. Ajanthan, and P. H. Torr, "Riemannian walk for incremental learning: Understanding forgetting and intransigence," in *Proc. Eur. Conf. Comput. Vis.*, 2018, pp. 532–547.

[26] J. Yoon, E. Yang, J. Lee, and S. J. Hwang, "Lifelong learning with dynamically expandable networks," 2017, *arXiv:1708.01547*.

[27] S. Yan, J. Xie, and X. He, "Der: Dynamically expandable representation for class incremental learning," in *Proc. IEEE/CVF Conf. Comput. Vis. pattern Recognit.*, 2021, pp. 3014–3023.

[28] Z. Li and D. Hoiem, "Learning without forgetting," *IEEE Trans. Pattern Anal. Mach. Intell.*, vol. 40, no. 12, pp. 2935–2947, Dec. 2018.

[29] S. Hou, X. Pan, C. C. Loy, Z. Wang, and D. Lin, "Learning a unified classifier incrementally via rebalancing," in *Proc. IEEE/CVF Conf. Comput. Vis. pattern Recognit.*, 2019, pp. 831–839.

[30] F.-Y. Wang, D.-W. Zhou, H.-J. Ye, and D.-C. Zhan, "Foster: Feature boosting and compression for class-incremental learning," in *Proc. Eur. Conf. Comput. Vis.*, 2022, pp. 398–414.

[31] A. Ashok, K. Joseph, and V. N. Balasubramanian, "Class-incremental learning with cross-space clustering and controlled transfer," in *Proc. Eur. Conf. Comput. Vis.*, 2022, pp. 105–122.

[32] F. Gao et al., "SAR target incremental recognition based on features with strong separability," *IEEE Trans. Geosci. Remote Sens.*, vol. 62, 2024, Art. no. 5202813.

[33] L. Wang, X. Yang, H. Tan, X. Bai, and F. Zhou, "Few-shot class-incremental SAR target recognition based on hierarchical embedding and incremental evolutionary network," *IEEE Trans. Geosci. Remote Sens.*, vol. 61, 2023, Art. no. 5204111.

[34] G. LI, J. Wang, C. Zhang, B. Feng, Y. Gao, and H. Yang, "Review of SAR image simulation methods," *Comput. Eng. Appl.*, vol. 57, no. 15, pp. 62–72, 2021.

[35] J. M. Arnold, L. J. Moore, and E. G. Zelnio, "Blending synthetic and measured data using transfer learning for synthetic aperture radar (SAR) target classification," *Proc. SPIE*, vol. 10647, pp. 48–57, 2018.

[36] J.-Y. Zhu, T. Park, P. Isola, and A. A. Efros, "Unpaired image-to-image translation using cycle-consistent adversarial networks," in *Proc. IEEE Int. Conf. Comput. Vis.*, 2017, pp. 2223–2232.

[37] C. Zhang, Y. Wang, H. Liu, Y. Sun, and L. Hu, "SAR target recognition using only simulated data for training by hierarchically combining CNN and image similarity," *IEEE Geosci. Remote Sens. Lett.*, vol. 19, 2022, Art. no. 4503505.

[38] Y. Sun, Y. Wang, L. Hu, and H. Liu, "SAR target recognition using simulated data by an ensemble multi-scale deep domain adaptation recognition framework," in *Proc. IEEE CIE Int. Conf. Radar (Radar)*, 2021, pp. 1413–1417.

[39] Q. He, L. Zhao, K. Ji, and G. Kuang, "SAR target recognition based on task-driven domain adaptation using simulated data," *IEEE Geosci. Remote Sens. Lett.*, vol. 19, 2022, Art. no. 4019205.

[40] M. Cha, A. Majumdar, H. Kung, and J. Barber, "Improving SAR automatic target recognition using simulated images under deep residual refinements," in *Proc. IEEE Int. Conf. Acoust., Speech Signal Process.*, 2018, pp. 2606–2610.

[41] L. Liu, Z. Pan, X. Qiu, and L. Peng, "SAR target classification with CycleGAN transferred simulated samples," in *Proc. IEEE Int. Geosci. Remote Sens. Symp.*, 2018, pp. 4411–4414.

[42] B. Camus, E. Monteux, and M. Vermet, "Refining simulated SAR images with conditional GAN to train ATR algorithms," in *Proc. Actes de la Conf. CAID*, 2020, pp. 160–167.

[43] M. Mirza and S. Osindero, "Conditional generative adversarial nets," 2014, *arXiv:1411.1784*.

[44] S. R. Sellers, P. J. Collins, and J. A. Jackson, "Augmenting simulations for SAR ATR neural network training," in *Proc. IEEE Int. Radar Conf. (RADAR)*, 2020, pp. 309–314.

[45] X. Zhang et al., "A method of improving the quality of SAR target electromagnetic simulation image based on scattering feature enhancement," *J. Signal Process.*, vol. 39, no. 9, pp. 1573–1586, 2023.

[46] X. Zhou, T. Tang, Y. Cui, L. Zhang, and G. Kuang, "Novel loss function in CNN for small sample target recognition in SAR images," *IEEE Geosci. Remote Sens. Lett.*, vol. 19, 2022, Art. no. 4018305.

Ziyang Tang received the B.S. degree in electronic information engineering from the University of Electronic Science and Technology of China, Chengdu, China, in 2022. He is currently working toward the M.S. degree in information and communication engineering with the State Key Laboratory of Complex Electromagnetic Environment Effects, National University of Defense Technology, Changsha, China.

His research interests include SAR ATR, incremental learning, and deep learning.

Yuli Sun received the Ph.D. degree in information and communication engineering from the National University of Defense Technology (NUDT), Changsha, China, in 2023.

He has authored or coauthored papers in IEEE TRANSACTIONS ON IMAGE PROCESSING, IEEE TRANSACTIONS ON NEURAL NETWORKS AND LEARNING SYSTEMS, IEEE TGRS, International Archives of the Photogrammetry, Remote Sensing and Spatial Information Sciences (ISPRS P&RS), *Pattern Recognition*, etc. He is currently a Postdoctor with the College of Aerospace Science and Engineering, NUDT. His research interests include remote sensing image processing and multitemporal image analysis.

Chenfang Liu received the M.S. degree in electronic information from the National University of Defense Technology, Changsha, China, in 2022. She is currently working toward the Ph.D. degree in information and communication engineering with the State Key Laboratory of Complex Electromagnetic Environment Effects, National University of Defense Technology, Changsha, China.

Her research interests include multisource image interpretation, feature extraction, and machine learning.

Yanjie Xu received B.S. and M.S. degrees in information and communication engineering from the National University of Defense Technology, Changsha, China, in 2018 and 2021. He is currently working toward the Ph.D. degree in information and communication engineering with the State Key Laboratory of Complex Electromagnetic Environment Effects, National University of Defense Technology.

His research interests include SAR ATR, incremental learning, and deep learning.

Lin Lei received the Ph.D. degree in information and communication engineering from the National University of Defense Technology, Changsha, China, in 2008.

She is currently a Professor with the School of Electronic Science, National University of Defense Technology. Her research interests include computer vision, remote sensing image interpretation, and data fusion.